

Reorientation transition of the magnetic proximity polarization in Fe/(Ga,Mn)As bilayersM. Sperl,¹ P. Torelli,² F. Eigenmann,¹ M. Soda,¹ S. Polesya,³ M. Utz,¹ D. Bougeard,¹ H. Ebert,³
G. Panaccione,² and C. H. Back¹¹*Institut für Experimentelle und Angewandte Physik, University of Regensburg, 93040 Regensburg, Germany*²*Consiglio Nazionale delle Ricerche-Istituto Officina dei Materiali (CNR-IOM), Laboratorio TASC, in Area Science Park, I-34149 Trieste, Italy*³*Department of Chemistry, Ludwig-Maximilians University Munich, 81377 München, Germany*

(Received 29 August 2011; revised manuscript received 31 January 2012; published 25 May 2012)

Recently, it has been observed that thin ferromagnetic Fe films deposited on top of (Ga,Mn)As layers induce a significant proximity polarization in the (Ga,Mn)As film even at room temperature. Furthermore, it was found that a thin interfacial region of the (Ga,Mn)As film is coupled antiferromagnetically to the Fe layer. Here we report a series of combined x-ray magnetic dichroism and superconducting quantum interference device magnetometer measurements for Fe/(Ga,Mn)As bilayers where the (Ga,Mn)As layer thickness is varied between 5 and 50 nm. We find a reorientation transition of the magnetic proximity polarization as a function of the (Ga,Mn)As thickness. The data are compared to results obtained performing *ab initio* calculations. A varying concentration of Mn interstitials as a function of (Ga,Mn)As layer thickness is responsible for this reorientation. Furthermore, exchange bias is studied in the fully epitaxial bilayer system. We find a rather strong ferromagnetic exchange bias. The strength of the exchange bias can be estimated by using a simple partial domain wall model.

DOI: [10.1103/PhysRevB.85.184428](https://doi.org/10.1103/PhysRevB.85.184428)

PACS number(s): 75.50.Pp, 75.30.Et, 78.20.Ls

The diluted magnetic semiconductor (DMS) GaMnAs is a promising material for semiconducting spintronic devices.¹ Since its first synthesis by Ohno *et al.*, progress has been made both in the understanding of the carrier-mediated mechanisms of the ferromagnetic (FM) state^{2–4} and in the ability to raise the Curie temperature T_C , mainly by postgrowth annealing.⁵ However, the record values of the Curie temperature seem to stagnate below 200 K⁶ with no clear strategy to further increase it above room temperature.

A novel route toward increasing the ordering temperature is to engineer the material using ferromagnetic metal overlayers. Tuning the magnetic properties at FM metal/DMS-based interfaces based on the most representative DMS system (Ga,Mn)As⁷ has recently been explored in a variety of experiments. For example, exchange bias is observed in MnAs/(Ga,Mn)As bilayers.^{8–10} In contrast, NiFe/(Ga,Mn)As bilayers show an independent magnetization behavior¹¹ with no exchange bias. In the Fe/(Ga,Mn)As system, the Fe overlayer induces a proximity polarization antiparallel to the Fe moment within a 1–2 nm (Ga,Mn)As region, which is promising for improving the ferromagnetic properties of very thin (Ga,Mn)As films.^{12–14} In fact, we have recently demonstrated that the proximity effect effectively enhances the operation temperature of Fe/(Ga,Mn)As hybrid spin injection devices when very thin (Ga,Mn)As injector and detector contacts are capped by an iron layer.¹⁵

However, to take full advantage of the control of the magnetization of the (Ga,Mn)As injector/detector contacts, it is of importance to understand the coupling mechanism in this epitaxial FM metal/DMS bilayer system. Here we map out the influence of the (Ga,Mn)As thickness in fully epitaxial Fe/(Ga,Mn)As heterostructures on the interfacial coupling as well as on the magnetization properties of the bulk layer by a combined study using element-specific x-ray magnetic circular dichroism (XMCD) measurements and bulk-sensitive superconducting quantum interference device (SQUID) magnetometry. By means of XMCD we are able

to identify a thickness dependent reorientation transition of the Mn magnetization from antiparallel to parallel alignment. Moreover, temperature-dependent XMCD and SQUID measurements show that for (Ga,Mn)As layer thicknesses below 15 nm the DMS system is fully ferromagnetically coupled to the Fe. For thicker (Ga,Mn)As layers we are able to identify a ferromagnetic exchange bias effect due to the presence of Fe on (Ga,Mn)As.

I. EXPERIMENTAL DETAILS

For the experiments (Ga,Mn)As films were grown on semi-insulating (001) GaAs substrates by LT MBE using a modified Veeco Gen II system. After heating of the epi-ready substrates to 600 °C in UHV to remove water and oxide from the surface, a 10-nm-thick LT-GaAs buffer layer was grown ($T \approx 200$ °C). Subsequently, the (Ga,Mn)As layers were deposited with Mn concentrations of $x = 0.06$ or $x = 0.12$ and different thicknesses from 3 to 35 nm. The growth rate for the low-temperature growth was below 0.3 Å/s. During deposition the growth temperature as well as the As/(Ga + Mn) ratio were kept constant at $T_{\text{growth}} = 234$ °C, As/(Ga + Mn) = 3.1:1 for 6% Mn and $T_{\text{growth}} = 181$ °C, As/(Ga + Mn) = 1.0:1 for 12% Mn. The nominal Mn concentration was determined by secondary ion mass spectroscopy (SIMS) measurements. The absolute Ga deposition rate was determined by reflection high-energy diffraction (RHEED) oscillation on (001) GaAs. Details on the (Ga,Mn)As growth and on the MBE system are given in Refs. 16–18.

Subsequently the samples were transferred to an attached metal MBE system without breaking the vacuum and 1.5 nm of Fe was epitaxially grown on all samples at room temperature to avoid interdiffusion. The Fe growth rate was controlled *in situ* by quartz monitors. Finally, the sample was covered with 4 nm of Au to prevent oxidation. By use of a mechanical shutter a part of the 2-inch wafer is covered during deposition of both metals to define an uncovered (Ga,Mn)As reference

area. The epitaxial quality was confirmed by cross-sectional transmission electron microscopy (TEM) studies revealing a smooth interface between Fe and (Ga,Mn)As.

The static magnetic properties of both the Fe/(Ga,Mn)As heterostructure and the (Ga,Mn)As reference layer were determined using a SQUID magnetometer. Moreover, XMCD experiments at the $L_{2,3}$ edges of Fe and Mn, on Fe/(Ga,Mn)As samples of different thicknesses, were carried out at the APE beamline of the Elettra Synchrotron (Trieste, Italy). The XMCD spectra as a function of the magnetization direction were acquired in total electron yield mode (TEY) by recording the drain current at remanence. The magnetization direction was reversed at each point of the XMCD spectra. During the experiment the incident light formed an angle of 45° with respect to the surface normal. Chemically resolved magnetic hysteresis loops of Fe and Mn were obtained by recording the value of the L_3 edge as a function of the applied magnetic field. This signal was subsequently divided by the same measurement obtained by fixing the photon energy 10 eV lower than the L_3 edge in order to remove artifacts due to influence of the stray fields on the secondary electrons. Both XMCD spectra and magnetic hysteresis loops were measured with opposite photon helicities, resulting in an inversion of the measured signals. In order to obtain a detectable signal of Fe and Mn in TEY, the sample was partially decapped from Au by controlled Ar-Ion sputtering *in situ* prior to the experiments. All samples were measured at room temperature, and the Fe/5 nm (Ga,Mn)As sample was also measured at 40 K.

II. RESULTS AND DISCUSSION

A. X-ray magnetic circular dichroism

In this experiment we measured XMCD spectra of Fe/(Ga,Mn)As samples with different thicknesses of the DMS film (ranging from 3 to 35 nm) and with different Mn concentrations, namely 6% and 12%. Measurements were performed at room temperature and at 40 K. In all samples the Fe film displays a large normalized XMCD signal around 30% at the L_3 edge after correction for the incident angle and degree of light polarization, indicating that the Fe layer is ferromagnetic and fully magnetized at remanence. The Mn $L_{2,3}$ edges display a ferromagnetic XMCD signal at

remanence in all measured samples as well, with a smaller XMCD signal with respect to Fe. The presence of a clear Mn magnetic signal at room temperature indicates that a small part of the (Ga,Mn)As layer, located at the interface, exhibits ferromagnetic order due to the proximity effect of the Fe layer, as already observed in previous experiments.^{12–14} In Fig. 1 XMCD spectra are displayed, which were recorded at room temperature at the Mn [Fig. 1(a)] and Fe [Fig. 1(b)] $L_{2,3}$ edges of a sample of 5 nm of (Ga,Mn)As thickness and 12% of Mn concentration. It is clearly visible that Fe displays the typical dichroism of bulk Fe with a normalized asymmetry value [defined as $(I^+ - I^-)/(I^+ + I^-)$ at the L_3 edge] close to 30% while Mn shows only a small dichroism of about 2%. Even though the magnitude and the shape of the XMCD of Fe and Mn is in perfect agreement with previous studies the sign of the coupling between the Fe and Mn is opposite to the one observed so far. In fact, an antiparallel alignment has always been observed at the Fe/(Ga,Mn)As interface, while the up-down feature of the XMCD of Fe and Mn in Figs. 1(a) and 1(b) clearly demonstrates parallel alignment of the Fe and Mn moments. This peculiar finding calls for further investigation of this effect. Indeed, the main difference between the sample studied here and previously studied samples is the thickness of the (Ga,Mn)As layer. Consequently, we performed a (Ga,Mn)As thickness-dependent XMCD study. To this end we measure a set of fully epitaxial Fe/(Ga,Mn)As samples with variable (Ga,Mn)As thickness (3, 5, 8, 10, 15, and 35 nm) and with a Mn concentration of 6% as well as 5 nm (Ga,Mn)As with films 12% Mn. The results are summarized in Fig. 1(c). Here we report the Mn XMCD asymmetry values where the negative and positive values indicate antiparallel and parallel alignment of the Mn magnetic moments with respect to the Fe moments, respectively. For (Ga,Mn)As films thicker than 15 nm we observe antiparallel coupling but for films of 10 nm and thinner the sign of the coupling is reversed and the coupling between the Fe and Mn moment is now ferromagnetic. We, further, investigate the properties of the ferromagnetic coupling as a function of an applied magnetic field along [110] direction and as a function of the temperature by measuring XMCD spectra at 40 K as well as chemically selective hysteresis loops. The XMCD spectra of Fe and Mn of the 12% Mn doped sample 5 nm thick (Ga,Mn)As recorded

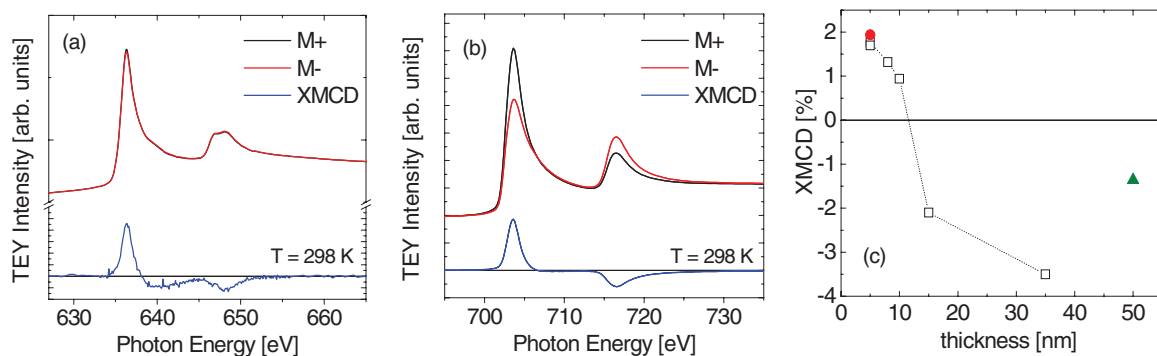


FIG. 1. (Color online) Fe and Mn $L_{2,3}$ XAS/XMCD spectra recorded at room temperature for Fe/(Ga,Mn)As heterostructures with 12% Mn: (a) Fe/5 nm (Ga,Mn)As measured at the Mn $L_{2,3}$ edge. (b) Fe/5 nm (Ga,Mn)As measured at the Fe $L_{2,3}$ edge. (c) Normalized Mn L_3 dichroism as a function of (Ga,Mn)As thickness for 6% Mn (black square) and for 5 nm (Ga,Mn)As, 12% Mn (red circle). The green triangle denotes the induced dichroism for 50 nm (Ga,Mn)As with 6% Mn (data taken from measurements of Ref. 13).

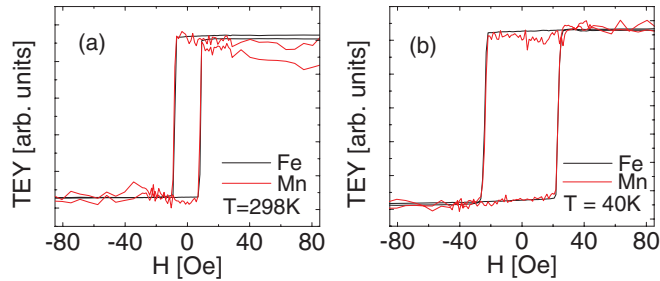


FIG. 2. (Color online) Element specific hysteresis loops with an in-plane field along [110] direction: (a) XMCD hysteresis loop measured at the Mn L_3 edge (red line) for Fe/5 nm (Ga,Mn)As with 12% Mn at room temperature normalized to the hysteresis loop measured at the Fe L_3 edge (black line). (b) XMCD hysteresis loop measured at the Mn L_3 edge (red line) normalized to the hysteresis loop measured at the Fe L_3 edge (black line) for the same sample at $T = 40$ K.

at 40 K are identical to the ones measured at room temperature except for the magnitude of the Mn XMCD asymmetry which is about 6% at low temperature. This is easily explained by the reduction of magnetization due to thermal fluctuations. In Figs. 2(a) and 2(b) the hysteresis loops recorded at the L_3 edges of Fe and Mn at room temperature and 40 K are reported. Fe displays a square hysteresis with coercive fields of 8 Oe at room temperature that increase up to 24 Oe at 40 K. The Mn signal (which has been normalized to the Fe

signal for better comparison) is a perfect copy of the iron signal demonstrating that the Mn polarization is totally dominated by the Fe magnetization.

To substantiate the experimentally observed ferromagnetic alignment of Fe and Mn moments we have performed a first-principles study of the GaAs/(Ga $_{1-x}$ Mn $_x$)As/Fe system using the spin polarized relativistic tight-binding KKR Green's function method.¹⁹ Exchange and correlation were treated within the framework of the local spin density approximation (LSDA) to the density-functional theory, using the parametrization of Vosko, Wilk, and Nusair.²⁰ The coherent potential approximation (CPA) is used to describe the substitutional disorder in (Ga,Mn)As.^{21,22} This allows us to avoid time-consuming supercell calculations and to use in the present case only two atoms per layer to construct the (Ga,Mn)As (001) surface. The calculations were performed for a semi-infinite geometry: eight monolayers of (Ga $_{1-x}$ Mn $_x$)As deposited on the GaAs (001) surface and covered with a one monolayer thick Fe film. The concentration x of Mn on the Ga sites was taken to be 5%.

Five different conditions on the interface with Fe were considered as follows: I, Ga terminated; II, Ga terminated with Mn interstitials at the interface; III, As terminated; IV, As terminated with Mn interstitials at the interface; and V, interface consisting of a single atomic plane of alternating Fe and As atoms.²³ On the basis of the obtained electronic structure the exchange interactions J_{ij} between magnetic atoms have been calculated using an approach suggested by Liechtenstein *et al.*²⁴

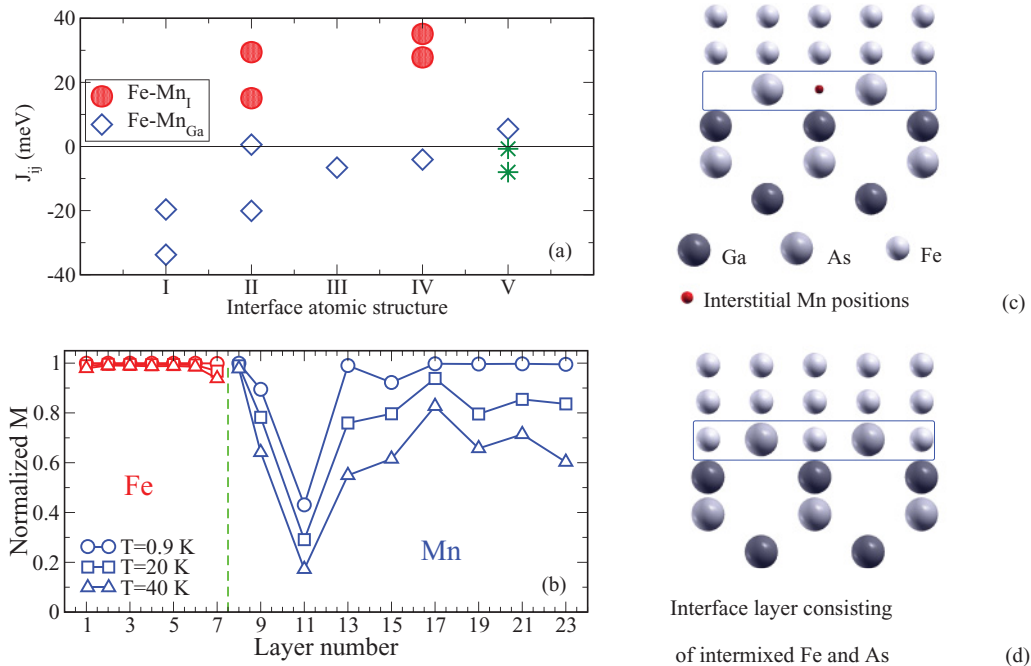


FIG. 3. (Color online) (a) Exchange coupling parameters J_{ij} between Fe and Mn atoms for five different atomic structures at the (Ga,Mn)As/Fe interface: I, Ga terminated; II, Ga terminated with Mn interstitials at the interface; III, As terminated; IV, As terminated with Mn interstitials at the interface; and V, interface consisting of a single atomic plane of alternating Fe and As atoms.²³ The stars (*) for structure V correspond to the interactions of Mn $_{\text{Ga}}$ from the interface with Fe atoms from the first fully occupied Fe layer. In each case, the parameters are given for the nearest-neighbor Mn $_{\text{Ga}}$ -Fe (Mn $_I$ -Fe) distances. (b) Results of Monte Carlo calculations: layer-resolved magnetization for a 7-ML Fe/8-ML (Ga $_{0.95}$ Mn $_{0.05}$)As bilayer with an As-terminated interface and Mn interstitials at the interface layer of (Ga,Mn)As (atomic structure IV). Each atomic layer is counted. In this case layer 8 contains As atoms. (c) Structure IV, the frame is around the interface layer. (d) Structure V, the AsFe layer at the interface is shown with the frame.

The results for the exchange interactions between Fe and Mn atoms at the interface are presented in Fig. 3(a). As one can observe that, for the Ga-terminated interface with only substitutional Mn (structure I), the exchange coupling between Mn_{Ga} (Mn on Ga sites) and Fe atoms at the interface is strongly antiferromagnetic. Moreover, the coupling between Mn_{Ga} within the (Ga,Mn)As film is ferromagnetic. As it was shown earlier (Ref. 11), this results in ferromagnetic order within the (Ga,Mn)As layers close to the Fe film up to room temperature. In the case of an As-terminated interface (structure III), the exchange interaction between Fe and Mn Ga atoms at the interface is also antiferromagnetic but weaker than in the case of a Ga termination. The magnetic coupling between Mn_{Ga} for the two layers close to the Fe films in this case is antiferromagnetic. The strength of this coupling is ~ 15.6 meV for Mn_{Ga} atoms lying within the same plane and ~ 11.5 meV for Mn from the neighboring planes. As a result, a disordered noncollinear magnetic structure is created within the (Ga,Mn)As layers close to the Fe film. Note that experimentally a mix of As- and Ga-terminated surfaces is most likely. In this case one can expect antiferromagnetic alignment of the average (Ga,Mn)As magnetization close to the interface with respect to the Fe film magnetization.

Theoretically, a different idealized interface structure was considered that is not observed experimentally. This surface structure consists of a single atomic plane of alternating Fe and As atoms [Fig. 3(d)], structure V in Fig. 3(a). The exchange coupling between Fe and Mn_{Ga} at the interface have rather small values in this case and the ferromagnetic Mn_{Ga} -Fe interaction with Fe atoms from the interface AsFe layer is compensated by the antiferromagnetic Mn_{Ga} -Fe coupling with Fe from the next to the interface fully occupied Fe layer. Thus, we can conclude that these interface atomic structures cannot be responsible for the ferromagnetic alignment of Fe and (Ga,Mn)As layers.

The exchange interaction changes strongly if Mn interstitials (Mn_I) are present at the interface layer of Fe/(Ga,Mn)As. The Mn atoms in the interstitial positions interact ferromagnetically with Fe atoms for both cases of Ga- and As-terminated interfaces [Fig. 3(a), structures II and IV). At the same time, the interaction between substitutional Mn with Fe is still antiferromagnetic but it is weaker. Despite the strong antiferromagnetic coupling between nearest-neighbor Mn_{Ga} and Mn_I magnetic moments, the orientation of the total Mn magnetic moment of the interface layer depends significantly on Mn-Fe interactions. As a result, ferromagnetic alignment of the Fe and Mn atoms at the interface will prevail. This is confirmed by Monte Carlo calculations. In Fig. 3(b) the layer-resolved normalized magnetization M for the As-terminated interface with Mn_I at the interface is shown for three temperatures, 0.9, 20, and 40 K. The concentration of Mn_I in the interface layer is equal to 10% and there is no interstitial Mn present in other layers. The concentration of Mn_{Ga} is 5%. All Mn atoms are randomly distributed on tetrahedral interstitial (for the interface layer) or Ga substitutional positions. The thermodynamic averaging was performed over 10 different disorder configurations. As one can see, the magnetization of Fe and (Ga,Mn)As films is aligned ferromagnetically. The reduced values of magnetization for layers 9 and 11 (corresponding to the first and second layers containing Mn_{Ga})

is a consequence of the disordered magnetic structure due to the Mn_{Ga} - Mn_I and Mn_{Ga} - Mn_{Ga} antiferromagnetic interactions in these layers. The transition to a paramagnetic state for the (Ga,Mn)As film occurs at around 50 K, while the layer nearest to the Fe layer (containing Mn interstitials) keeps ferromagnetic order well above room temperature due to the strong coupling to the Fe film. For the Ga-terminated interface ferromagnetic alignment of the average magnetization of (Ga,Mn)As and Fe films was also obtained. But, in this case, the disordered magnetic structure that reduces the average magnetization is established in the (Ga,Mn)As nearest to the Fe film. It should be also mentioned that for the As-terminated interface the concentration of 5% of Mn_I could result in ferromagnetic orientation of the average magnetization of a (Ga,Mn)As layers with respect to the Fe film magnetization. The obtained results are fully consistent with the experimental data and ferromagnetic alignment between Mn and Fe atoms is explained by the presence of interstitial Mn in the vicinity of the Fe film.

We attribute the observed change in relative orientation of magnetization at the interface between Fe and Mn to a change in Mn interstitial concentration in dependence of the (Ga,Mn)As thickness. For thick (250–300 nm) layers of (Ga,Mn)As Koeder *et al.* have found a pronounced decrease of the carrier concentration from the surface toward the (Ga,Mn)As/GaAs interface due to a nonhomogeneous distribution of point defects like Mn interstitials or As antisites in the layer.²⁵ Moreover, it is found that for film thicknesses less than 10 nm, the diffusion length of Mn_I in the film is comparable to the film thickness.^{5,26}

For thin (Ga,Mn)As layers this is manifested by a high amount of randomly distributed Mn at the surface represented by a surface oxide layer. For thicker (Ga,Mn)As layers, on the other hand, an increasing Mn interstitial concentration away from the surface is found.²⁶ In our case, a chemical passivation of Mn interstitials in a surface oxide layer is not likely since the (Ga,Mn)As film was directly overgrown with Fe after preparation. This may lead to a significant increased number of Mn interstitials at the interface between Fe and (Ga,Mn)As and, consequently, to a reorientation of the induced magnetization at the interface with reduced (Ga,Mn)As thickness.

B. Magnetometry

For magnetic characterization SQUID magnetometry is performed on Au/Fe/(Ga,Mn)As/GaAs(001) as well as on reference (Ga,Mn)As/GaAs(001) samples for all (Ga,Mn)As thicknesses and Mn concentrations (6% and 12%). Figure 4(a) shows a major hysteresis loop at 20 K for a Fe/(Ga,Mn)As heterostructures with a (Ga,Mn)As thickness of 30 nm and Mn concentration of 12% and field applied along the [110] crystal axis. This corresponds to an easy axis of the Fe layer for the chosen Fe thickness. The magnetic moment is not normalized to the sample volume since the bilayer stack consists of two different ferromagnetic layers. A distinct two-step switching process is observed for Fe on 20 and 30 nm (Ga,Mn)As with 6% Mn and Fe/30 nm (Ga,Mn)As with 12% Mn for all temperatures below T_C of (Ga,Mn)As. Interestingly, the two-step switching is absent in the case of Fe/30 nm

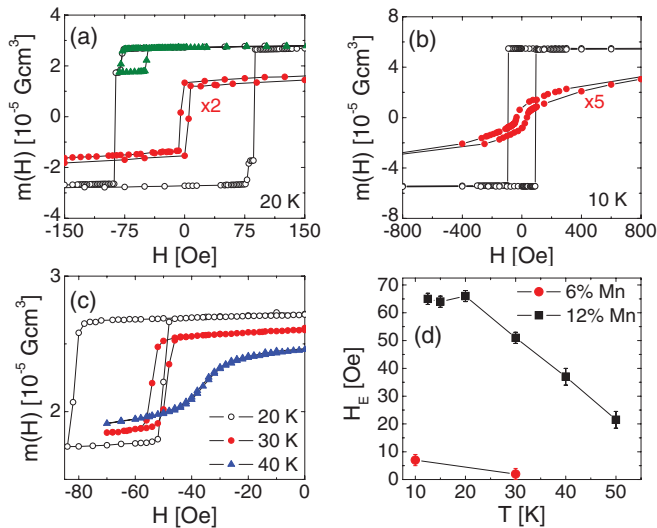


FIG. 4. (Color online) (a) Major magnetization loop $m(H)$ along (Ga,Mn)As [110] measured at $T = 20$ K for a bilayer Fe/30 nm (Ga,Mn)As sample with 12% Mn showing a distinct two-step switching process (open circles); minor magnetization loop after saturating the Fe layer (red solid circles). (b) SQUID measurement of the field dependence of the magnetic moment $m(H)$ for Fe/5 nm (Ga,Mn)As, 12% Mn (open circles) and the corresponding (Ga,Mn)As reference (red solid circles) along [110] measured at 10 K. (c) Minor magnetization loops for Fe/30 nm (Ga,Mn)As with 12% Mn measured along [110] for different temperatures. (d) Dependence of the exchange field H_E on temperature for Fe/30 nm (Ga,Mn)As with 12% Mn (black squares) and 6% Mn (red circle).

(Ga,Mn)As with 12% Mn at the lowest measuring temperature (10 K). By comparison to the (Ga,Mn)As reference sample and hysteresis loops above T_C of (Ga,Mn)As, we can assign the smaller coercive field to (Ga,Mn)As and the second switching process to Fe. The situation changes considerably if the (Ga,Mn)As thickness is reduced. Remarkably, for Fe/ x nm (Ga,Mn)As ($x = 5, 8, 10, 12, 15$ nm), no separate switching field for Fe and (Ga,Mn)As can be observed in the whole temperature range below the T_C of (Ga,Mn)As. Corresponding data are shown in Fig. 4(b) for Fe/5 nm (Ga,Mn)As with 12% Mn. The single switching event is determined by the coercive field of the Fe film, which means there is a mutual switching of Fe and (Ga,Mn)As defined by the magnetization reversal of Fe. This ferromagnetic coupling between both magnetic layers in the integral SQUID measurements is in agreement with the element-specific XMCD hysteresis measurement (Fig. 2). For the Fe/30 nm (Ga,Mn)As samples (6% and 12% Mn) we measured minor loops as a function of temperature to determine the exchange field. The minor loops were measured by saturating the sample in a positive magnetic field and subsequently demagnetizing the sample in a negative field large enough to switch the (Ga,Mn)As layer but smaller than the coercive field of Fe. Figures 4(a) and 4(c) shows the minor loops for three different temperatures for Fe/30 nm (Ga,Mn)As with 12% Mn; clearly a displacement of the center of the minor loop can be observed. The shift is opposite to the magnetization of the Fe layer for all measured temperatures indicating an exchange bias that is ferromagnetic. The observed exchange field is roughly 65 Oe at the lowest measurement

temperature of 12.5 K [Fig. 4(d)] and one order of magnitude smaller for Fe/30 nm (Ga,Mn)As with 6% Mn. The evidence of ferromagnetic exchange bias is seemingly in contrast to our observation of an antiparallel alignment (thickness (Ga,Mn)As ≥ 15 nm) of the two layers at the interface^{12,13} and to the observation of an antiferromagnetic exchange bias effect in recent SQUID measurements of Fe/(Ga,Mn)As bilayer samples.¹⁴ Interestingly, a ferromagnetic coupling was also reported by Wilson *et al.* for MnAs/(Ga,Mn)As¹⁰ but without the possibility to study the relative orientation of magnetization at the interface.

To calculate the exchange field experienced by (Ga,Mn)As in the evaluated bilayer system we use a simple model proposed by Mauri *et al.* to describe exchange bias systems²⁷ and successfully adopted to calculate the exchange field of hard/soft ferromagnetic bilayers.^{10,28} Here it is considered that the magnetization of the Fe layer is fixed and aligned along its easy axis in the positive [110] direction of (Ga,Mn)As. At the interface within a thin layer ($d \approx 1-2$ nm) the magnetization of GaMnAs is aligned antiparallel to the Fe magnetization up to a field of 50 kOe, as it was deduced from recent measurements.^{12,13} Subsequently, the magnetization of the (Ga,Mn)As is free to rotate toward the global easy axis of (Ga,Mn)As. In the presence of a cubic and uniaxial anisotropy the direction of the bulk (Ga,Mn)As easy axis with respect to the [110] direction is given by (the other easy axis is located symmetrically with respect to the [110] direction):

$$\sin \varphi = \sqrt{(K_C - K_U)/2K_C}. \quad (1)$$

Here K_C and K_U denote the cubic and the uniaxial anisotropy constant. We assume that a partial domain wall (PDW) of thickness t_1 will nucleate in the (Ga,Mn)As film away from the interfacial coupled layer. A sketch for the exchange coupled Fe/(Ga,Mn)As bilayer is given in Fig. 5.

Considering a thin interfacial layer antiparallel to Fe and a typical domain wall width of ~ 40 nm²⁹ we assume $t_2, d \ll t_1 \approx t_{GMA}$ [t_{GMA} : thickness of the (Ga,Mn)As film]. Using

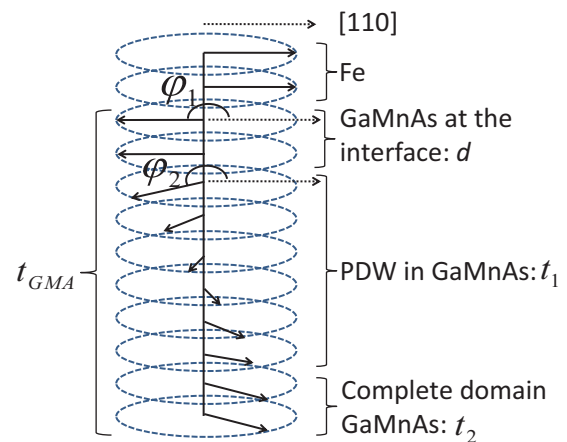


FIG. 5. (Color online) Schematic representation of a partial domain-wall configuration in (Ga,Mn)As. Directly at the interface an interfacial layer with thickness d of (Ga,Mn)As is aligned antiparallel with respect to Fe. The arrows represent the spin direction, which continuously rotates with increasing distance from the interface. At a certain distance t_1 , a complete domain with thickness t_2 is formed.

this approximation the energy density per unit area can be expressed by¹⁰

$$E = 2\sqrt{AK_{\text{eff}}}(\cos\varphi_1 - \cos\varphi_2) - \frac{A_{\text{ex}}}{d}\cos\varphi_1 + K_U t_{\text{GMA}} \sin^2\varphi_2 + \frac{1}{4}K_C t_{\text{GMA}} \cos^2 2\varphi_2 - H M t_{\text{GMA}} \cos\varphi_2. \quad (2)$$

The first term represents the energy of the PDW determined by the spin stiffness constant A and the effective anisotropy K_{eff} , and φ_1 is the angle between the magnetization of Fe and the induced magnetization in (Ga,Mn)As at the interface and φ_2 is the angle between the Fe layer and the easy axis of the bulk GaMnAs. The second term (A_{ex}) denotes the interfacial exchange energy and the third and fourth terms are the energy of the uniaxial (K_U) and the biaxial (K_C) anisotropies. The last term describes the Zeeman energy in an external field H with the (Ga,Mn)As saturation magnetization M . Due to the strong antiferromagnetic interface coupling between Fe and (Ga,Mn)As, the angle $\varphi_1 = 180^\circ$. According to the Stoner-Wohlfarth coherent rotation model,³⁰ one obtains, by energy minimization ($\frac{\partial^2 E}{\partial \varphi_2^2} > 0$),

$$H_{\text{ex}} = -2\sqrt{AK_{\text{eff}}}/M t_{\text{GMA}}$$

as an expression for the exchange field.¹⁰

To compute the exchange field, we used literature data for (Ga,Mn)As, in terms of the spin stiffness $A = 4 \times 10^{-8}$ erg/cm,²⁹ the uniaxial anisotropy constant $K_U = -1.1 \times 10^3$ erg/cm³, and the cubic anisotropy constant $K_C = 2.2 \times 10^3$ erg/cm³.³¹ Because of the strong cubic anisotropy we can consider $K_{\text{eff}} \approx K_C/4$.²⁹ The (Ga,Mn)As saturation magnetization was determined by SQUID to be $M = 38$ G (at $T = 12.5$ K) for 12% Mn and 18 G (at $T = 10$ K) for 6% Mn (both 30 nm thickness). This yields for $t_{\text{GMA}} = 30$ nm an exchange bias of $H_{\text{ex}} = -82$ Oe at 12.5 K (12% Mn) and $H_{\text{ex}} = -174$ Oe at 10 K (6%). Although this is only a very crude model, the calculated exchange bias shows reasonable agreement with our measurement on Fe/30 nm (Ga,Mn)As with 12%, whereas it overestimates the exchange field (for the

corresponding magnetization) of Fe/30 nm (Ga,Mn)As with 6% Mn by a factor of 10. In order to get a full understanding of whether this deviation is due to the limitations of the partial domain wall model, one would have to determine all material parameters like spin stiffness and (temperature-dependent) anisotropy constants for each individual sample, which was not in the focus of this work.

Further investigations were performed concerning the temperature dependence of the exchange bias field H_E . Figure 4(d) shows that the exchange field decreases nearly linearly with increasing temperature. At first glance, an increase of the exchange field is expected because of the reduced magnetization at higher temperatures. But, as already reported by Wilson *et al.* this discrepancy can be explained within the partial domain wall model, assuming the temperature dependence of the anisotropy,^{29,32,33} which may overcome that of the magnetization with increasing temperature.¹⁰

C. Summary

In summary, we present XMCD and SQUID data on a series of fully epitaxial Fe/(Ga,Mn)As bilayers with different (Ga,Mn)As film thicknesses and Mn concentrations. We find an unusual transition from ferromagnetic to antiferromagnetic coupling of the interfacial Mn moments to the Fe moments. The data can be corroborated with the help of *ab initio* calculations where the influence of the increasing density of interstitial Mn at the interface is taken into account for thinner (Ga,Mn)As layers. In addition, we study exchange bias in these fully epitaxial bilayers and find rather strong ferromagnetic exchange bias. Using a simple partial domain wall model, the magnitude of the exchange bias can be estimated. Our findings may prove to be helpful when engineering the magnetization direction of thin (Ga,Mn)As layers, which can show induced ferromagnetism at room temperature due to the proximity polarization and which can be used for spin injection devices.

ACKNOWLEDGMENTS

This work has been supported by the Deutsche Forschungsgemeinschaft (DFG) via SFB689. We acknowledge ELETTRA for provision of synchrotron radiation facilities.

¹T. Dietl, *Nat. Mater.* **9**, 965 (2010).

²H. Macdonald, P. Schiffer, and N. Samarth, *Nature (London)* **4**, 195 (2005).

³T. Dietl, H. Ohno, and F. Matsukura, *Phys. Rev. B* **63**, 195205 (2001).

⁴A. Kaminski and S. Das Sarma, *Phys. Rev. Lett.* **88**, 247202 (2002).

⁵K. W. Edmonds, P. Bogusławski, K. Y. Wang, R. P. Campion, S. N. Novikov, N. R. S. Farley, B. L. Gallagher, C. T. Foxon, M. Sawicki, T. Dietl, M. Buongiorno Nardelli, and J. Bernholc, *Phys. Rev. Lett.* **92**, 037201 (2004).

⁶L. Chen, S. Yan, P. F. Xu, J. Lu, W. Z. Wang, J. J. Deng, X. Qian, Y. Ji, and J. H. Zhao, *Appl. Phys. Lett.* **95**, 182505 (2009).

⁷T. Jungwirth, J. Sinova, J. Mašek, J. Kučera, and A. H. MacDonald, *Rev. Mod. Phys.* **78**, 809 (2006).

⁸M. Zhu, M. J. Wilson, B. L. Sheu, P. Mitra, P. Schiffer, and N. Samarth, *Appl. Phys. Lett.* **91**, 192503 (2007).

⁹M. Zhu, M. J. Wilson, P. Mitra, P. Schiffer, and N. Samarth, *Phys. Rev. B* **78**, 195307 (2008).

¹⁰M. J. Wilson, M. Zhu, R. C. Myers, D. D. Awschalom, P. Schiffer, and N. Samarth, *Phys. Rev. B* **81**, 045319 (2010).

¹¹S. Mark, C. Gould, K. Pappert, J. Wenisch, K. Brunner, G. Schmidt, and L. W. Molenkamp, *Phys. Rev. Lett.* **103**, 017204 (2009).

¹²F. Maccherozzi, M. Sperl, G. Panaccione, J. Minár, S. Polesya, H. Ebert, U. Wurstbauer, M. Hochstrasser, G. Rossi, G. Woltersdorf,

- W. Wegscheider, and C. H. Back, *Phys. Rev. Lett.* **101**, 267201 (2008).
- ¹³M. Sperl, F. Maccherozzi, F. Borgatti, A. Verna, G. Rossi, M. Soda, D. Schuh, G. Bayreuther, W. Wegscheider, J. C. Cezar, F. Yakhou, N. B. Brookes, C. H. Back, and G. Panaccione, *Phys. Rev. B* **81**, 035211 (2010).
- ¹⁴K. Olejnik, P. Wadley, J. A. Haigh, K. W. Edmonds, R. P. Campion, A. W. Rushforth, B. L. Gallagher, C. T. Foxon, T. Jungwirth, J. Wunderlich, S. S. Dhesi, S. A. Cavill, G. van der Laan, and E. Arenholz, *Phys. Rev. B* **81**, 104402 (2010).
- ¹⁵C. Song, M. Sperl, M. Utz, M. Ciorga, G. Woltersdorf, D. Schuh, D. Bougeard, C. H. Back, and D. Weiss, *Phys. Rev. Lett.* **107**, 056601 (2011).
- ¹⁶U. Wurstbauer, M. Sperl, D. Schuh, G. Bayreuther, J. Sadowski, and W. Wegscheider, *J. Cryst. Growth* **301**, 260 (2007).
- ¹⁷U. Wurstbauer, M. Sperl, M. Soda, D. Neumaier, D. Schuh, G. Bayreuther, J. Zweck, and W. Wegscheider, *Appl. Phys. Lett.* **92**, 102506 (2008).
- ¹⁸M. Reinwald, U. Wurstbauer, M. Döppe, W. Kipferl, K. Wagenhuber, H.-P. Tranitz, D. Weiss, and W. Wegscheider, *J. Cryst. Growth* **278**, 690 (2005).
- ¹⁹H. Ebert and R. Zeller, SPR-TB-KKR package (2006), <http://olymp.cup.uni-muenchen.de/ak/ebert/SPR-TB-KKR>.
- ²⁰S. H. Vosko, L. Wilk, and M. Nusair, *Can. J. Phys.* **58**, 1200 (1980).
- ²¹M. Matsumoto, J. B. Staunton, and P. Strange, *J. Phys.: Condens. Matter* **2**, 8365 (1990).
- ²²W. H. Butler, *Phys. Rev. B* **31**, 3260 (1985).
- ²³T. J. Zega, Aubrey T. Hanbicki, S. C. Erwin, I. Zutić, G. Kioseoglou, C. H. Li, B. T. Jonker, and R. M. Stroud, *Phys. Rev. Lett.* **96**, 196101 (2006).
- ²⁴A. I. Liechtenstein, M. I. Katsnelson, V. P. Antropov, and V. A. Gubanov, *J. Magn. Magn. Mater.* **67**, 65 (1987).
- ²⁵A. Koeder, S. Frank, W. Schoch, V. Avrutin, W. Limmer, K. Thonke, R. Sauer, A. Waag, M. Krieger, K. Zuern, P. Ziemann, S. Brotzmann, and H. Bracht, *Appl. Phys. Lett.* **82**, 3278 (2003).
- ²⁶K. M. Yu, W. Walukiewicz, T. Wojtowicz, J. Denlinger, M. A. Scarpulla, X. Liu, and J. K. Furdyna, *Appl. Phys. Lett.* **86**, 042102 (2005).
- ²⁷D. Mauri, H. C. Siegmann, P. S. Bagus, and E. Kay, *J. Appl. Phys.* **62**, 3047 (1987).
- ²⁸Z. J. Guo, J. S. Jiang, J. E. Pearson, S. D. Bader, and J. P. Liu, *Appl. Phys. Lett.* **81**, 2029 (2002).
- ²⁹A. Sugawara, H. Kasai, A. Tonomura, P. D. Brown, R. P. Campion, K. W. Edmonds, B. L. Gallagher, J. Zemen, and T. Jungwirth, *Phys. Rev. Lett.* **100**, 047202 (2008).
- ³⁰E. C. Stoner and E. P. Wohlfarth, *Philos. Trans. R. Soc. London A* **240**, 599 (1948).
- ³¹F. Hoffmann, G. Woltersdorf, W. Wegscheider, A. Einwanger, D. Weiss, and C. H. Back, *Phys. Rev. B* **80**, 054417 (2009).
- ³²M. Cubukcu, H. J. von Bardeleben, K. Khazen, J. L. Cantin, M. Zhu, M. J. Wilson, P. Schiffer, and N. Samarth, *J. Appl. Phys.* **105**, 07C506 (2009).
- ³³M. Sawicki, F. Matsukura, A. Idziaszek, T. Dietl, G. M. Schott, C. Rueter, C. Gould, G. Karczewski, G. Schmidt, and L. W. Molenkamp, *Phys. Rev. B* **70**, 245325 (2004).